Ram, S., Prabhat, P., Ward, E. S., and Ober, R. J. Dual objective fluorescence microscopy for single molecule imaging applications. In *Three-Dimensional and Multidimensional Microscopy: Image Acquisition and Processing XVI. SPIE International Society for Optical Engineering*, 7184: 7184-0C, 2009.

Dual objective fluorescence microscopy for single molecule imaging applications

Sripad Ram[1], Prashant Prabhat[1,2], E. Sally Ward[1] and Raimund J. Ober[1,2]

[1]Department of Immunology, University of Texas Southwestern Medical Center, Dallas, TX, 75390, [2]Department of Electrical Engineering, University of Texas at Dallas, Richardson, TX, 75083.

ABSTRACT

Fluorescence microscopy is an invaluable tool for studying biological processes in cells. In the recent past there has been significant interest in imaging cellular processes at the single molecule level. Single molecule experiments remove ensemble averaging effects and provide information that is typically not accessible through bulk experiments. One of the major requirements in single molecule imaging applications is that a sufficient number of photons be detected from the single molecule. This is not only important for the visual identification of single molecules, but also plays a crucial role in the quantitative analysis of the acquired data. Here, we demonstrate the use of a dual objective imaging configuration for single molecule studies. The configuration uses two opposing objective lenses, where one of the objectives is in an inverted position and the other objective is in an upright position. The use of opposing objective lenses has been previously demonstrated in 4pi confocal microscopy and I5M to achieve high axial resolution when compared to confocal/widefield microscopes. Here we demonstrate that the dual objective imaging configuration provides higher photon collection efficiency when compared to a regular microscope for a given illumination condition. As a result, single molecules can be localized with better accuracy when imaged through opposing objective lenses than when imaged through a regular optical microscope. Analytical tools are introduced to estimate the 2D location of single molecules and to characterize the accuracy with which they can be determined.

Keywords: Multifocal plane microscopy, 3D single molecule tracking, localization accuracy, Fisher information matrix

1. INTRODUCTION

Single particle tracking is a powerful tool to study biological processes at the cellular and molecular level.[1,2] The recent past has witnessed a dramatic increase in the use of single particle/molecule imaging, where several new techniques have been reported to image and track single particles/molecules in two and three dimensions at nanoscale precision and resolution.[3–12] In single particle/molecule imaging applications the number of detected photons from the labeled entity plays a crucial role in the analysis of the acquired data. For instance, it has been shown by us[4,13] and others[14–16] that the 2D localization accuracy of the nanoprobe (i.e., accuracy with which the 2D location of a nanoprobe can be determined) is inversely proportional to the square root of the number of detected photons. This inverse square root dependence has also been reported for the 3D localization accuracy problem.[17,18] In the resolution problem, which deals with resolving distances between two point sources, the accuracy with which the distance between two point sources can be determined in 2D/3D has been shown to be inversely proportional to the square root of the number of detected photons.[6,19] Hence achieving a high photon collection efficiency is important in such studies.

Currently, single particle/molecule imaging experiments are typically carried out either on an inverted or an upright microscope, in which an objective lens illuminates the sample and also collects the fluorescence signal from it. Note that although fluorescence emission from the sample occurs in all directions (i.e., above and below the sample), the use of a single objective lens in these microscope configurations results in collecting light from only one side of the sample. Even if a high numerical aperture objective lens is used, not all photons emitted

at one side of the sample can be collected due to the finite collection angle of the objective lens. Hence, even under the best imaging conditions, inverted/upright microscopes collect only a fraction of the photons emitted from the sample.

Here we report the use of a microscope configuration that uses two opposing objective lenses for imaging individual fluorescent nanoprobes. We refer to this configuration as dual objective multifocal plane microscopy (dMUM). In dMUM, one of the objectives is in an inverted position, while the other objective is in an upright position (see Figure 1). The sample, which is placed between the two objectives, is illuminated in widefield mode through one of the objective lenses, analogous to the way the sample is illuminated in a standard microscope, and the emitted fluorescence from the sample is collected through both objective lenses. Hence for a given illumination condition, dMUM detects the fluorescence from above and below the sample, and as a result collects more photons from the sample than a standard microscope.

The use of opposing objective lenses is not new and has been reported previously, for example, in the implementation of 4pi confocal microscopy[20, 21] and I5M[22, 23] Recently, there has been a proposal for using opposing objective lenses for generating a three-dimensional lattice of focal spots with the potential for 3D imaging applications.[24] The dMUM configuration reported here is demonstrated for single particle/molecule imaging applications, in particular to improve the photon collection efficiency. On the one hand, the focal planes of the two objectives can be positioned to image the same plane within the sample for 2D imaging. Alternately, the focal planes can be positioned to simultaneously image different planes within the sample, which was recently shown by us to be beneficial for 3D tracking of subcellular objects[8, 25] and single molecules[8, 26] in live cells.

2. RESULTS

2.1 Dual objective multifocal plane microscopy

The dMUM configuration proposed here enables the imaging of the sample from both the top and the bottom. Our specific implementation of dMUM used two inverted Zeiss microscopes (AxioObserver). One of the microscopes ('top scope') was mounted in an 'upside down' orientation on linear X-Y translation stages which were attached to the other microscope ('bottom scope'). The sample was placed in the bottom scope and the objective in the top scope was attached to the nose piece through C-mount spacers in order for it to reach the sample. The sample is illuminated in widefield mode through the bottom scope. The fluorescence light from the sample is collected by objective lenses in the top and bottom scope and passes through emission filters. In each microscope, the collected fluorescence signal is focused onto a CCD camera. Prior to acquiring images from the sample, the top scope is aligned with the help of the translation stages to ensure that the objectives of the top and bottom scopes image the same field of view in the sample. Figure 2 shows a dMUM image of a QD sample, which were acquired in our setup.

2.2 Photon collection efficiency of dMUM

The dual objective imaging capability of dMUM enables collecting more photons from the sample than with a standard microscope configuration. To verify the improved light collection efficiency of dMUM, we calculated the number of detected photons from the nanoprobes in the acquired data (Figure 2). Because of the use of different objectives and cameras in the top and bottom scopes, for a given nanoprobe the number of photons detected were different in the two scopes. For example, for the QD highlighted with an arrowhead in Figure 2, 8700 photons and 3100 photons were collected from the top and bottom cameras, respectively, when the exposure time of both cameras was 300 ms. Note that a higher photon count is observed in the top camera although a lower NA objective is used in the top scope. This is due to the fact that the quantum efficiency of the camera in the top scope is higher than the quantum efficiency of the camera in the bottom scope.

2.3 2D location estimation from dMUM images

We have developed a new algorithm to determine the 2D location of nanoprobes from dMUM images. The algorithm simultaneously fits a pair of Airy profiles to the dMUM image of a nanoprobe. We tested our algorithm on several nanoprobe images that were acquired by imaging a stationary nanoprobe sample in our dMUM imaging setup. For comparison purposes, the 2D location of the nanoprobe was also independently determined from the

TOP SCOPE

CAMERA

TUBE LENS

MIRROR

EMISSION FILTER

OBJECTIVE LENS

SAMPLE

OBJECTIVE LENS

DICHROIC MIRROR

EXCITATION LIGHT

CAMERA

EMISSION FILTER

MIRROR

TUBE LENS
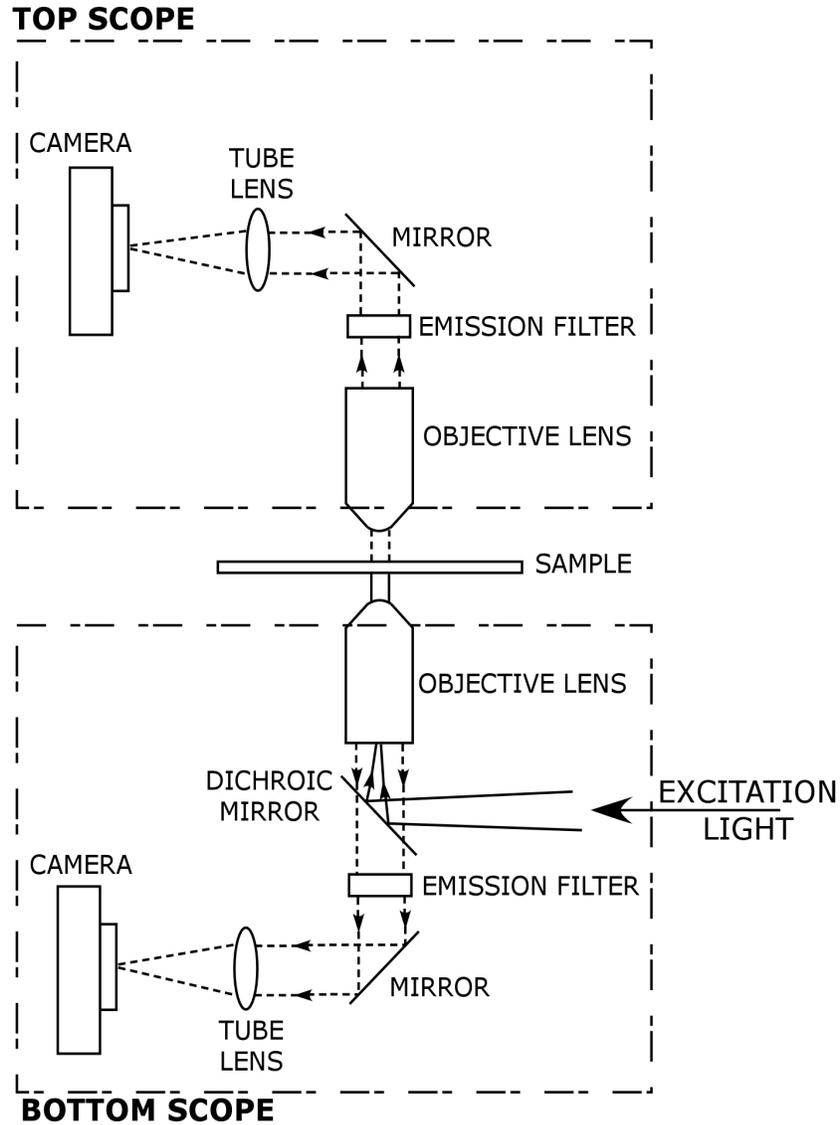
BOTTOM SCOPE

Figure 1. Dual objective multifocal plane microscopy. The figure shows the schematic of a dual objective multifocal plane microscope than can simultaneously image the sample from top and bottom. Our specific implementation of the dMUM imaging configuration used two inverted microscopes (Zeiss AxioObserver), where one of the microscopes (top scope) was in an upside down orientation and mounted on linear translation stages, which were then attached to the other microscope (bottom scope).
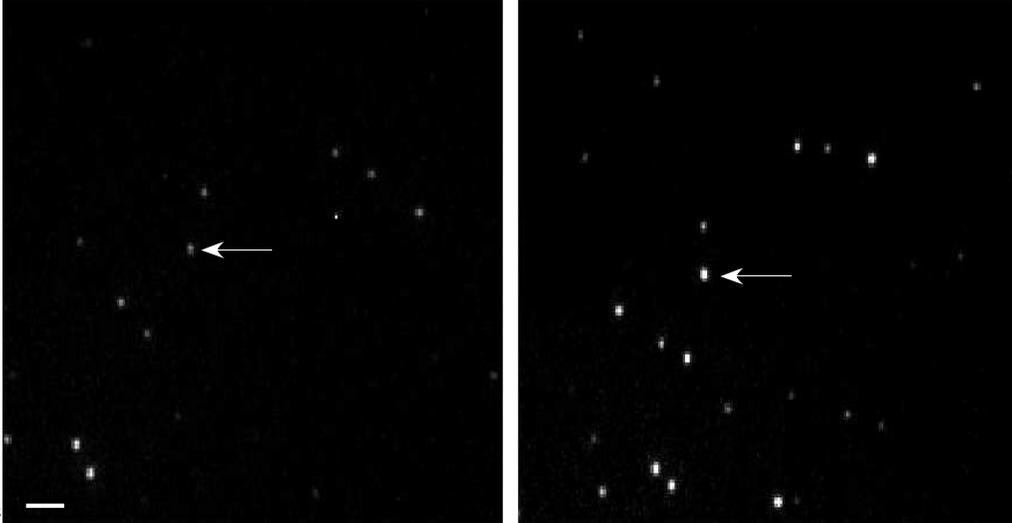
Figure 2. dMUM images of A nanoprobe sample. The figure shows the bottom plane (left) and top plane (right) image of a sample containing QD655 labels adsorbed on a coverslip. For the QD label highlighted with an arrow, the number of detected photons in the bottom plane and top plane images are 3100 and 8700, respectively. Scale bar = $1\mu m$.

image acquired from the top (bottom) scope only. This was done by independently fitting Airy profiles to the data acquired from the top and bottom scopes. Our analysis showed that the accuracy (standard deviation) of the 2D location estimates from dMUM is consistently better than when the 2D location is estimated from only the top or the bottom scope images. In particular, we saw that the X-Y accuracy for dMUM is about 20% - 35% better than the X-Y accuracy for the top/bottom scope. For example, for one of the nanoprobes that we analyzed, the accuracy of determining the X (Y) coordinate of the nanoprobe from dMUM images is 3.81 nm (3.34 nm). For the same nanoprobe, the accuracy of independently determining the X (Y) coordinate from the top scope and bottom scope images are 5.38 nm (5.43 nm) and 4.79 nm (4.32 nm), respectively.

2.4 2D localization accuracy limits for dMUM images

In the previous section, we showed that our estimation algorithm can extract the 2D location of the nanoprobes from dMUM images. We next wanted to quantify the best possible accuracy that can be obtained for a given dataset. In many practical situations, knowing the best possible accuracy that can be attained is of importance, for example, to evaluate the feasibility of carrying out a particular experiment or to assess the performance of a particular estimation algorithm. Here, we have carried out a statistical analysis based on the Fisher information matrix, which provides a quantitative measure of the total information contained in the acquired data about the parameters that we wish to estimate. Specifically, we calculate the 2D localization measure for dMUM and for a standard microscope. The 2D localization measure provides a limit to the accuracy with which the 2D location of the nanoprobe can be determined. A small numerical value of the localization measure implies high accuracy in determining the location, while a large numerical value of the localization measure implies poor accuracy in determining the location.

The analytical expression of the Fisher information matrix for the 2D location estimation problem for dMUM is given by

$$\mathbf{I}(\theta) = \mathbf{I}_t(\theta) + \mathbf{I}_b(\theta), \quad \theta \in \Theta, \tag{1}$$

where Θ denotes the parameter space, $\mathbf{I}_t(\theta)$ ($\mathbf{I}_b(\theta)$) denotes the Fisher information matrix for the image acquired in the top (bottom) scope. The analytical expressions for $\mathbf{I}_t(\theta)$ and $\mathbf{I}_b(\theta)$ are analogous to those of a standard microscope, which has been published before for the 2D location estimation problem (see[4]).

We calculated the 2D localization measure for the nanoprobes whose X-Y location was determined from dMUM images and independently from the top and bottom scopes images. For all the nanoprobes that we analyzed, we found that the accuracy of the X/Y coordinates were consistently close to the 2D localization

measure for all the microscope configurations. For example, for the specific nanoprobe whose X-Y accuracies aree listed in Section 2.3 the 2D localization measure of the X/Y coordinate for the dMUM configuration, the top scope and the bottom scope are 3.54 nm, 5.73 nm and 4.49 nm, respectively, which are in close agreement to the corresponding X-Y accuracies. This shows that our estimation algorithm indeed attains the best possible accuracy.

REFERENCES

1. M. J. Saxton and K. Jacobson, "Single particle tracking : applications to membrane dynamics," *Annual Review in Biophysics and Biomolecular Structure* **26**, pp. 373–399, 1997.
2. X. Michalet, A. N. Kapanidis, T. Laurence, F. Pinaud, S. Doose, M. Pflughoefft, and S. Weiss, "The power and prospects of fluorescence microscopies and spectroscopies," *Annual Review of Biophysics and Biomolecular Structure* **32**, pp. 161–182, 2003.
3. G. J. Schütz, J. Hesse, G. Freudenthaler, V. P. Pastushenko, H.-G. Knaus, B. Pragl, and H. Schindler, "3d mapping of individual ion channels on living cells," *Single Molecules* **2**, pp. 153–157, 2000.
4. R. J. Ober, S. Ram, and E. S. Ward, "Localization accuracy in single molecule microscopy," *Biophysical Journal* **86**, pp. 1185–1200, 2004.
5. M. P. Gordon, T. Ha, and P. R. Selvin, "Single molecule high resolution imaging with photobleaching," *Proceedings of the National Academy of Sciences USA* **101**(17), pp. 6462–6465, 2004.
6. S. Ram, E. S. Ward, and R. J. Ober, "Beyond Rayleigh's criterion: A resolution measure with application to single-molecule microscopy," *Proceedings of the National Academy of Sciences USA* **103**, pp. 4457–4462, 2006.
7. K. A. Lidke, B. Rieger, T. M. Jovin, and R. Heintzmann, "Superresolution by localization of quantum dots using blinking statistics," *Optics Express* **13**(18), pp. 7052–7062, 2005.
8. P. Prabhat, Z. Gan, J. Chao, S. Ram, C. Vaccaro, S. Gibbons, R. J. Ober, and E. S. Ward, "Elucidation of intracellular pathways leading to exocytosis of the Fc receptor, FcRm, using multifocal plane microscopy," *Proceedings of the National Academy of Sciences USA* **104**, pp. 5889–5894, 2007.
9. L. Holtzer, T. Meckel, and T. Schmidt, "Nanometric three-dimensional tracking of individual quantum dots in cells," *Applied Physics Letters* **90**, p. 053902, 2007.
10. E. Betzig, G. H. Patterson, R. Sougrat, O. W. Lindwasser, S. Olenych, J. S. Bonifacino, M. W. Davidson, J. Lippincott-Schwartz, and H. F. Hess, "Imaging intracellular fluorescent proteins at nanometer resolution," *Science* **313**, pp. 1642–1645, 2006.
11. A. Sharonov and R. M. Hochstrasser, "Wide-field subdiffraction imaging by accumulated binding of diffusing probes," *Proceedings of the National Academy of Sciences* **103**, pp. 18911–18916, 2006.
12. J. G. Ritter, R. Veith, J. P. Siebrasse, and U. Kubitscheck, "High-contrast single-particle tracking by selective focal plane illumination microscopy," *Optics Express* **16**, pp. 7142–7152, 2008.
13. S. Ram, E. S. Ward, and R. J. Ober, "A stochastic analysis of performance limits for optical microscopes," 2006.
14. N. Bobroff, "Position measurement with a resolution and noise limited instrument," *Review of Scientific Instruments* **57**(6), pp. 1152–1157, 1986.
15. U. Kubitscheck, O. Kückmann, T. Kues, and R. Peters, "Imaging and tracking single GFP molecules in solution," *Biophysical Journal* **78**, pp. 2170–2179, 2000.
16. R. E. Thompson, D. R. Larson, and W. W. Webb, "Precise nanometer localization analysis for individual fluorescent probes," *Biophysical Journal* **82**, pp. 2775–2783, 2002.
17. S. Ram, E. S. Ward, and R. J. Ober, "How accurately can a single molecule be localized in three dimensions using a fluorescence microscope?," *Proceedings of the SPIE* **5699**, pp. 426–435, 2005.

18. F. Aguet, D. V. D. Ville, and M. Unser, "A maximum likelihood formalism for sub-resolution axial localization of fluorescent nanoparticles," *Optics Express* **13**, pp. 10503–10522, 2005.

19. J. Chao, S. Ram, A. V. Abraham, E. S. Ward, and R. J. Ober, "Resolution in three-dimensional microscopy," *Optics Express* , Submitted.

20. S. Hell and E. H. K. Stelzer, "Properties of a 4Pi confocal fluorescence microscope," *Journal of the Optical Society of America A* **9**, pp. 2156–2166, 1992.

21. S. Hell and E. H. K. Stelzer, "Fundamental improvement of resolution with a 4Pi-confocal fluorescence microscope using two-photon excitation," *Optics Communicaitons* **93**, pp. 277–282, 1992.

22. M. G. L. Gustafsson, D. A. Agard, and J. W. Sedat, "Sevenfold improvement of axial resolution in 3D widefield microscopy using two objective lenses," *Proceedings of the SPIE* **2412**, pp. 147–156, 1995.

23. M. Gustafsson, "Extended resolution fluorescence microscopy," *Current Opinion in Structural Biology* **9**, pp. 627–634, 1999.

24. E. Betzig, "Excitation strategies for optical lattice microscopy," *Optics Express* **13**, pp. 3021–3036, 2005.

25. P. Prabhat, S. Ram, E. S. Ward, and R. J. Ober, "Simultaneous imaging of different focal planes in fluorescence microscopy for the study of cellular dynamics in three dimensions," *IEEE Transactions on Nanobioscience* **3**(4), pp. 237–242, 2004.

26. S. Ram, P. Prabhat, J. Chao, E. S. ward, and R. J. Ober, "High accuracy 3d quantum dot tracking with multifocal plane microscopy for the study of fast intracellular dynamics in live cells," *Biophysical Journal,* In Press .